

Laboratory Measurements of Dispersion Relation and Damping Coefficients for Whistler Waves

Andrew Kent^{1†}

¹Department of Physics and Astronomy, University of California, Los Angeles

March 2020

A overview of the data collected by launching RF waves into a magnetized, cold, argon plasma. Time varying changes in the plasma were measured via a "B-dot Probe", whose data led to the analysis of the dispersion relation and damping rate (Γ). An investigation of backwards and forwards resonance also occurred.

1. Introduction

Whistler waves have been studied for over 100 years now, they were first heard likely as early as the 1880's, but the earliest description is attributed to Barkhausen (1919). Though it was Storey in his 1953 paper "An investigation of whistling atmospherics" who correctly showed that the whistling sounds being detected were attributed to lightning discharges Storey (1953).

Whistler waves are produced on Earth as a result of lightning discharges which will excite several frequencies along the magnetic field lines of the Earth. The reason for their namesake is due to early detections using broadband spectrograms, the particular characteristic is that the tone of the signal quickly descends like a train whistle. While there is much to learn about whistler waves, the aspect of them focused on in this paper will be the interesting structure of their index of refraction which also includes spatial damping as well as a look at forwards and backwards perpendicular propagation.

The structure of the equations describing the index of refraction for our cold plasma is originally attributed to Appleton (1924), though the form we will be digesting will be more familiar to a generalization due to Sen & Wyller (1960). To investigate the theoretical predictions we will be launching radio frequency (RF) waves in a Gaussian packet using an antenna situating along the main axis of the plasma in our device (Figure 1), we will then be measuring the time varying magnetic field produced by the wave to determine wave characteristics.

2. Theory

2.1. Wave Packet Dispersion

Our objective will be to launch RF waves at a certain frequency from our antenna at the back of the plasma chamber, in order to experimentally test the dispersion relation of our plasma. There is a hitch though, our wave will in-fact be time-localized and so as a result there will be some spread due to dispersion. A short general refresher of wave packet dispersion will follow which will approximate what our antenna is sending into

† Email address for correspondence: andrewkent@ucla.edu

our plasma. To begin, let us consider a simple taylor expansion to our dispersion relation (for a carrier frequency of k_c)

$$\omega(k) = \omega(k_c) + (k - k_c)\omega'(k_c) + \frac{1}{2}(k - k_c)^2\omega''(k_c) + \dots \quad (2.1)$$

which can be written as

$$\omega(k) = k_c v_p + (k - k_c)v_g + \frac{1}{2}(k - k_c)^2\Gamma + \dots \quad (2.2)$$

With this expansion we can write a Gaussian wave-packet carrying a frequency k_c as

$$A(x, t=0) = f(x) = e^{-\frac{1}{2\sigma^2}(x-x_0)^2} e^{ik_c x} \quad (2.3)$$

where σ is the half-max-width of our Gaussian and x_0 is the initial position. Taking the Fourier transform

$$\tilde{f}(x) = \frac{\sigma}{2\sqrt{\pi}} e^{-\frac{\sigma_x^2}{2}(k-k_c)^2} e^{ix_0(k-k_c)} \quad (2.4)$$

so then

$$A(x, t) = \frac{\sigma}{2\sqrt{\pi}} \int e^{i(kx - [k_c v_p + (k - k_c)v_g + \frac{1}{2}(k - k_c)^2\Gamma]t)} e^{-\frac{\sigma_x^2}{2}(k-k_c)^2} e^{ix_0(k-k_c)} dk \quad (2.5)$$

whose result is

$$A(x, t) = \exp \left(-\frac{1}{2} \left(\frac{x - (x_0 + v_g t)}{\sqrt{\sigma_x^2 - i\Gamma t}} \right)^2 \right) e^{ik_c x} e^{-ik_c t(v_g - v_p)} \quad (2.6)$$

which can we can rewrite as

$$A(x, t) = \exp \left(-\frac{1}{2} \left(\frac{x - (x_0 + v_g t)}{\sigma(t)} \right)^2 \right) e^{i\phi(x, t)} \quad (2.7)$$

so, the thing to note is that the packet will begin to broad due to the term:

$$\sigma(t) = \sigma_x \sqrt{1 + \frac{\Gamma^2}{\sigma^4} t^2} \quad (2.8)$$

Note that this packet is centered at $x_0 + v_g t$, i.e. the center of the Gaussian moves with the group velocity. Roughly speaking, the spatial extent of the pulse grows in real space as

$$\Delta x \sim \Delta x_0 + \frac{d^2\omega(k_c)}{dk^2} \frac{t}{\Delta x_0} \quad (2.9)$$

an effect called "pulse dispersion", which we will attempt to see in our experimental device.

2.2. Dispersion Relation for Whistler Wave

The main results for the dispersion relation for our whistler wave will be summarized below, for a fuller explanation refer to "The Fundamental's of Plasma Physics" by Bittencourt (2013). For a right handed circularly polarized wave propagating in the parallel direction with respect to the background magnetic field, we expect to find the following dispersion relation for an undamped wave is

$$n_{\parallel}^2 \sim \frac{\omega_{pe}^2}{\omega} \frac{1}{|\Omega_e| - \omega} \quad (2.10)$$

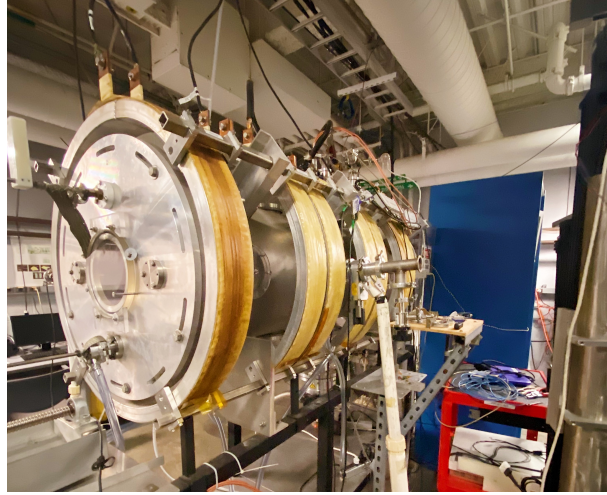


FIGURE 1. Experimental device, 1.5 m long and 0.4 m in diameter. A vacuum is achieved with a turbo pump, then argon gas is let in to fill the chamber at a set pressure.

where n_{\parallel} is the index of refraction in the parallel direction, ω_{pe} is the plasma frequency and Ω_e is the cyclotron frequency for the electrons. This expression can be simplified to be written as

$$\omega \sim |\Omega_e| \frac{k_{\parallel}^2 \delta_e^2}{1 + k_{\parallel}^2 \delta_e^2} \quad (2.11)$$

where $\delta_e = c/\omega_{pe}$ and k_{\parallel} is the wave-number in the parallel direction.

2.3. Spatial Wave Damping

If one allows a drag term in the equations, one can show the following dispersion relation

$$n_{\parallel}^2 \sim \frac{\omega_{pe}^2}{\omega} \frac{1}{|\Omega_e| - (\omega + i\nu)} \quad (2.12)$$

where k_{\parallel} will now be written as $k_{\parallel} = k_{\parallel,r} + i\kappa$. Therefore we will have the following expression for the dispersion relation

$$\omega \sim |\Omega_e| \frac{(k_{\parallel,r} + i\kappa)^2 \delta_e^2}{1 + (k_{\parallel,r} + i\kappa)^2 \delta_e^2} \quad (2.13)$$

3. Experimental Setup

3.1. Experimental Device

The device is seen in Figure 1, it is a large cylindrical solenoid which allows for uniform magnetic fields inside to be on the order of 50 Gauss. The plasma density we were working with we found to be $n_e = 7.1 * 10^{16} 1/m^3$ at the center of our plasma column, while the typical plasma temperature we found was between 1 and 3 electron volts (eV).

3.2. Timing in the Experimental Device

The RF pulse is sent down the barrel of the device in the afterglow, and measurements are taken with a time period of about a microsecond, as a result of this short time period

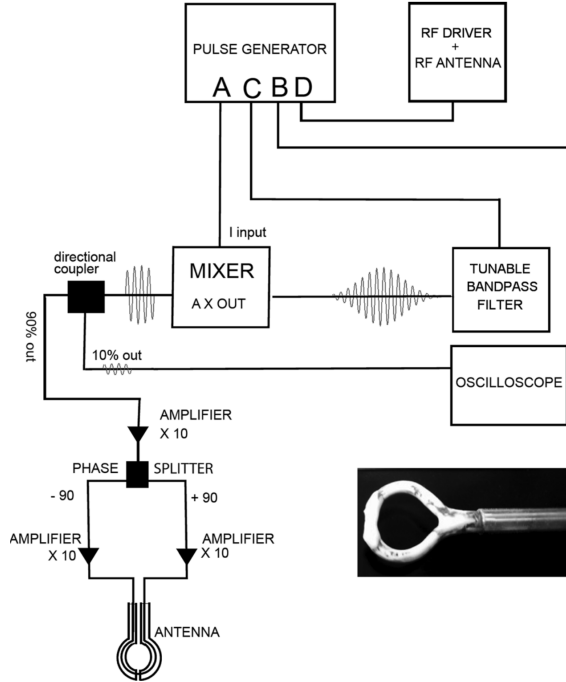


FIGURE 2. Electronics diagram for experiment

for data taking the measurements received on the digital oscilloscope at nanosecond intervals.

3.3. Electronic Set-up of Device

The probe is placed into the device by skewering it down the axis, and is allowed to slide into the plasma via a sliding seal lock at the interface on the wall of the device. In addition to being able to control the extent of the probe in the plasma, the probe can also rotate in the theta direction with an additional motor. The data from the three components of the b-dot probe are then relayed to the digital oscilloscope in addition to data from a photo-diode on one of the windows of the device which allows us to see when the plasma is "on". For most of our data runs, we varied the extent to which the probe was in our plasma between 10 and 60 cm, and rotated our probe between angles of -6 and 6 degrees. Though for one of our measurements we extended angles to much farther out to -28 and 28 degrees. The diagram for the device and electronics is shown in Figure 2.

3.4. Three Axis B-Dot Probe

B-dot probes are some of the oldest and most well known sensors for picking up time varying magnetic fields. The basic premise behind how they operate is based on Faraday's law of electromagnetic induction. But because the b-dot probe can be subject to electrical oscillations the signal received by the probe cannot always be trusted. For further information about how one goes about reducing/removing the oscillations relating to the internal circuit structure as well as solutions to other b-dot measuring issues refer to Bose *et al.* (2018). In our experiment we will be working with a three directional b-dot

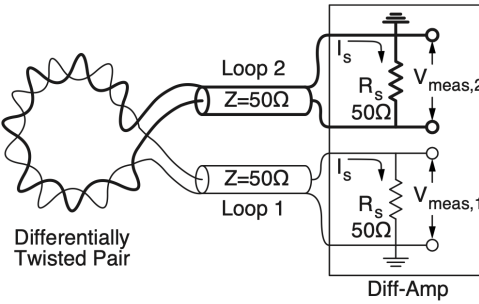


FIGURE 3. Circuit diagram for one of the axes of the loop. Everson *et al.* (2009)

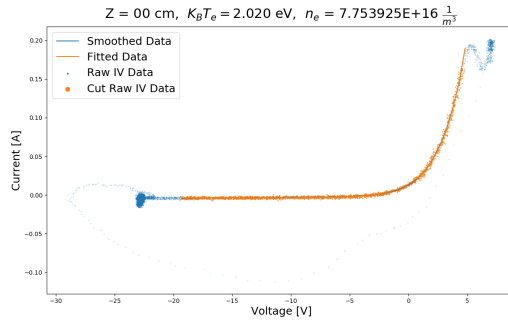


FIGURE 4. IV trace at the center of the plasma column

probe, whose circuit diagram for each loop is show in Figure 3. This design was made to study fast transient effects in what are called "exploding plasmas" Everson *et al.* (2009).

In this experiment we will be collecting information about the change in the magnetic field of our whistler wave, from this data we will be able to reconstruct the shape of the wave to then infer the dispersion relation and other properties of our wave.

4. Results

4.1. Plasma Temperature and Density

Following the procedure learned in lab #2, we took IV trace data in our plasma, and found that the density varied between 4 and $7 \times 10^{16} \text{ } 1/m^3$ while our electron temperature likewise was found between the values of 1.5 and 2.1 electronvolts (eV). These results were calculated using a langmuir probe which we were able to place at different distances from the center of the plasma. The results of these calculations are seen in Figure 4 for the IV trace at the center of the plasma and Figure 5 for the edge.

4.2. Dispersion Relation

Seen in Figure 6, we see a high degree of agreement for our experimental measurements of the wavelength versus the initial RF frequency, though we notice that the first four measurements are displaying an odd pattern. At this moment it is not known whether there was an issue with the fitting of our whistler wave, if there was a mistake with labeling our data, if this is in-fact what happened in the experiment or etc.

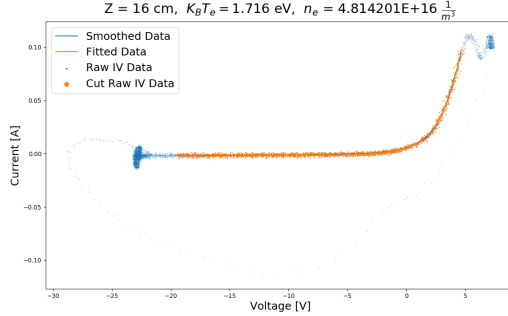


FIGURE 5. IV trace 16 cm from the center of the plasma column

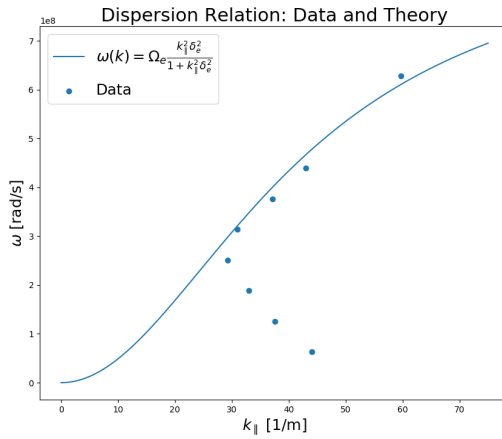


FIGURE 6. Dispersion relation for a variety of RF frequencies

4.3. Wave Reflection in Chamber?

Because the whistler waves damp out before traveling the extent of the chamber, I was unable to see any reflections back into the chamber. The graph showing the damping rate for different RF frequencies is seen in Section (4.6).

4.4. Dispersion Relation for Single Pulse

The goal of sending the pulse into the plasma was to try and see if we would be able to "see" higher frequencies arriving at the probe first, though when viewing the movie in Figure 7 we see a wave whose crests do not change as it travels along the length of the device. Therefore we were unable to extract the relevant information necessary to get a dispersion relation from a single pulse.

4.5. Propagation across the Magnetic Field?

In all of the data collected for this lab, we were unable to see evidence of propagation across the magnetic field. Evidence for this effect could have been possibly seen in a spreading of the wave as the wave travels down the extent of the device, though in all the movies created using our data there was little to no evidence of this phenomena occurring.

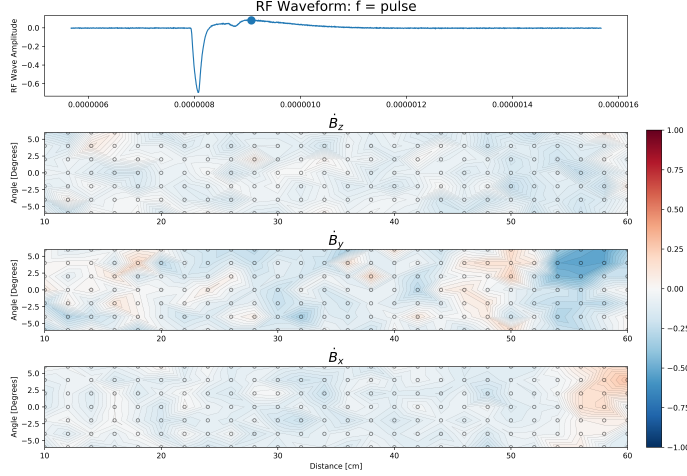
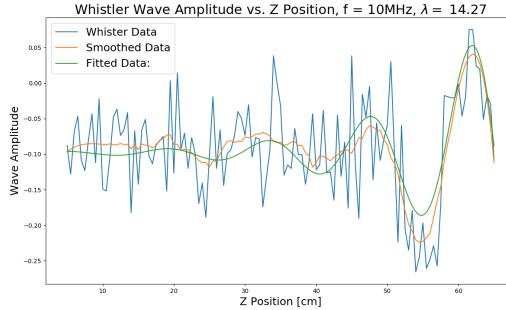


FIGURE 7. Plasma response to pulse signal

FIGURE 8. Damping along extent of device, for $\theta = 0$ and $f = 10\text{MHz}$

4.6. Spatial Wave Damping Γ , plot of Damping as a function of RF Frequency $\Gamma(f)$

In figures 8, 9 and 10 we see the raw, smoothed and fitted curves associated to the whistler wave propagating down the extent of the device at an instant in time. I have chosen three of the 8 different frequencies we launched down the device, notice how much cleaner the fit is for Figure 10 for the highest frequency than the lower frequencies. This reason alone may be the reason for why we notice some strange behaviors for the lowest four frequencies on the dispersion relation graph, that there was simply too much noise to make an accurate analysis for those data runs.

In the calculations for the fit of the damped curves we found the coefficient which governs this damping, and plotted these values against the theoretical curve in 11.

We see some agreement, in fact one of our data points lies on the theoretical value—though beyond that the similarities are not many.

4.7. Backwards and Forwards Propagation

As seen in Figure 12, we have evidence of a backwards perpendicular propagation, a phenomena predicted by solving for the dispersion relation for an oblique incident wave. We were able to see this phenomena in this case because for our last data measurements we took a very wide angle (-28 to 28 degrees), where before we were limiting ourselves

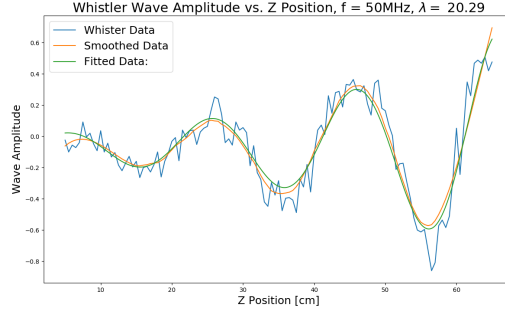


FIGURE 9. Damping along extent of device, for $\theta = 0$ and $f = 50\text{MHz}$

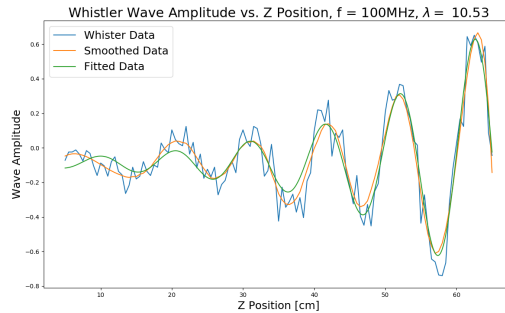


FIGURE 10. Damping along extent of device, for $\theta = 0$ and $f = 100\text{MHz}$

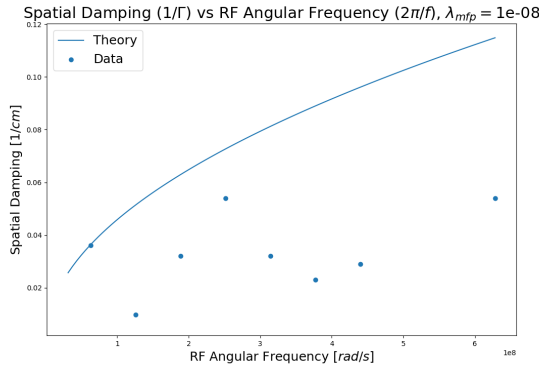


FIGURE 11. Damping parameter κ , theory and data

to 6 plus and minus- therefore we were unable to determine the regime when one would find either forward or backwards propagation.

5. Conclusion and Summary

In this report we found that the dispersion relation predicted by a cold, parallel propagating whistler wave model agreed with experiments when considering frequencies above 50 MHz. Additionally we found evidence of the backwards perpendicular phase

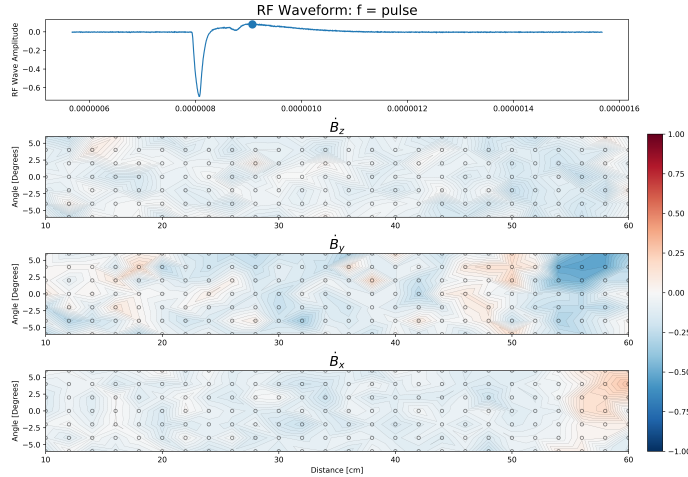


FIGURE 12. Backwards perpendicular propagation

speed, although this was mostly due to luck because it was our last run and we decided to get a very large and rich data set which we were not able to get for the other runs due to time constraints.

6. Acknowledgments

I would very much like to thank Professor Troy Carter for his care and attention throughout the quarter in teaching our Physics 180E Plasma Laboratory class, and also our TA's Quinn Pratt and Gurleen Bal for their assistance with all things physics. This has been a wonderful class to cap off my undergraduate career at UCLA, especially one which connects so many different topics.

REFERENCES

- APPLETON, EDWARD V 1924 Geophysical influences on the transmission of wireless waves. *Proceedings of the Physical Society of London* **37** (1), 16D.
- BARKHAUSEN, H 1919 Two phenomena revealed with the help of new amplifiers. *Phys. Z* **29** (6), 401–403.
- BITTENCOURT, JOSÉ A 2013 *Fundamentals of plasma physics*. Springer Science & Business Media.
- BOSE, SAYAK, KAUR, MANJIT, BARADA, KSHITISH K, GHOSH, JOYDEEP, CHATTOPADHYAY, PRABAL K & PAL, RABINDRANATH 2018 Understanding the working of a b-dot probe. *European Journal of Physics* **40** (1), 015803.
- EVERSON, ET, PRIBYL, P, CONSTANTIN, CG, ZYLSTRA, A, SCHAEFFER, D, KUGLAND, NL & NIEMANN, C 2009 Design, construction, and calibration of a three-axis, high-frequency magnetic probe (b-dot probe) as a diagnostic for exploding plasmas. *Review of Scientific Instruments* **80** (11), 113505.
- SEN, HK & WYLLER, AA 1960 Generalization of the appleton-hartree magneto-ionic formula. *Physical Review Letters* **4** (7), 355.
- STOREY, LRO 1953 An investigation of whistling atmospherics. *Philosophical Transactions of the Royal Society of London. Series A, Mathematical and Physical Sciences* **246** (908), 113–141.